

## Improvement of Algorithms for On-line Interdigital Dielectrometry Measurement of Material Properties

A.V. Mamishev, C. Lin, Y. Du, B.C. Lesieutre, and M. Zahn

Massachusetts Institute of Technology

Department of Electrical Engineering and Computer Science

Laboratory for Electromagnetic and Electronic Systems

Cambridge, MA 02139

**Abstract:** Interdigital frequency-wavenumber dielectrometry is useful for a variety of industrial applications where standard parallel plate measurements are either impossible or do not provide sufficient information about the studied dielectric. This paper describes a practical model-based approach to the estimation of physical parameters through one-side access measurement of dielectric properties of solid and liquid insulators.

The focus of this study is improvement of the speed, precision, and reliability of previously developed algorithms. The inverse problem of material parameter estimation is solved through interpolation of the parametric sweeps of the variables of interest. As a result, the need for a computationally expensive iterative solution of the forward problem is eliminated.

### Introduction

Improvement of both theoretical and experimental techniques related to  $\omega$ - $k$  (frequency-wavenumber) dielectrometry has been a research goal for over a decade. A conceptual approach and a mathematical model were developed in the early eighties [1,2]. Further studies revealed noticeable discrepancies between the model and the experimental results. Consequently, the mechanical design, electronic circuitry, and modeling techniques were revised to achieve better performance of interdigital dielectrometry sensors [3].

This paper continues these studies by introducing a self-calibrating model-based approach for the estimation of the complex dielectric permittivity. The algorithm exploited in presented experiments is suitable for real-time measurements. The parameter estimation takes less than a second because the calculated response of the sensor to the variation of dielectric permittivity is computed in advance using finite-element software.

### Motivation

The complex dielectric permittivity of insulating materials can be mapped to many other physical properties, such as concentration of moisture and impurities, density, porosity, presence of cracks and dendrites, etc. Potential applications of the technology are numerous, including monitoring of manufacturing processes, dynamics of diffusion, aging, and structural deformation. Although the measurement procedures are fairly simple, the quantification and interpretation of the measurement results can be quite challenging.

### Theoretical Background

Multi-wavelength  $\omega$ - $k$  dielectrometry is based on the use of periodically alternating coplanar interdigitated electrodes. Such geometry eliminates the need for parallel-plate cells, which is advantageous in cases when only one side of the test material is accessible and for measurements of spatial profiles of dielectric properties.

The depth of penetration of the electric field into the material above the plane of the electrodes is proportional to the spacing between the electrodes. Measuring interelectrode admittances for pairs of electrodes with different spacing provides information about the properties of materials at different distances from the surface of the dielectric. With appropriate algorithms, information about the spatial distribution of dielectric properties and dependent physical variables in the tested material can be obtained.

### Description of the Sensor

The fabrication technology for interdigital sensors varies depending on the application, working environment, linear dimensions, and required precision of manufacturing. The sensor used in this study was designed for on-line measurement of dielectric properties of standard solid and liquid dielectric materials.

Figure 1 shows the top view of the sensor. It comprises three sets of interdigitated electrodes with spatial wavelengths of 1.0 mm, 2.5 mm, and 5.0 mm etched on a common flexible Teflon substrate. Each wavelength has a separate guard plane on the back of the substrate, shown in shaded gray, and guard fingers, which approximate the effect of infinite periodicity in the  $Y$  direction. Electronic circuitry described in previous publications measures interelectrode transcapacitance and transconductance at frequencies ranging from 0.005 Hz to 10 kHz [3].

Although the substrate is flexible, and the copper electrodes are only 14  $\mu\text{m}$  thick, the sensor cannot completely conform to all surface irregularities. The finite thickness of the electrodes also contributes to the formation of the air cavities between the sensor and the tested material, as shown in Figure 2. The fluids, on the other hand, fill all cavities completely. Because of that, the properties of liquids and the properties of solid

materials are evaluated with different parameter estimation algorithms.

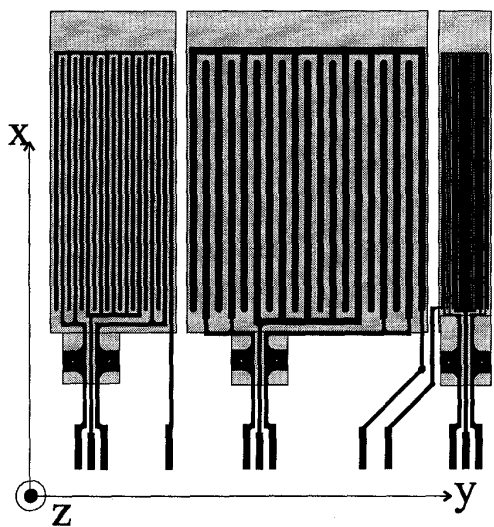


Figure 1. The three-wavelength interdigital sensor.

### Calibration

Teflon, being a chemically inert and hydrophobic material, was chosen for the substrate. However, the mechanical properties of Teflon are less attractive than those of some other polymers: cold flow, thermal expansion, and softness, although moderate, limit the precision of the geometric dimensions of the electrodes. In addition, erosion, friction, and corrosion slightly reduce the width and thickness of the electrodes with time. Because of all these factors, the average metallization ratio, defined here as the ratio of the sum of the widths of the drive and sense electrodes to the wavelength can rarely be exactly the designed 50%. In our experience, the metallization ratio, found from microscope photographs, varied from 45% to 55%.

The presented algorithm requires that the metallization ratio,  $\beta$ , is found by the calibration of the sensor in air prior to measurements. This is done for each wavelength by locating the measured interelectrode capacitance  $C_{12}$  on the precomputed curve representing a functional dependence  $C_{12}(\beta)$ . Figure 3 shows this dependence for all three wavelengths for a teflon substrate with relative permittivity of 2.1 and thickness  $254 \mu\text{m}$ . These functions were computed with high precision using finite-element software Maxwell by Ansoft Corp. The functional form of each curve shown in Figure 3 is approximated with the following expression:

$$\beta = a_2 \sqrt{C_{12}} + a_1 C_{12} + a_0, \quad (1)$$

where the empirical coefficients found by the best fit for each wavelength with  $C_{12}$  having units of pF are listed in Table 1.

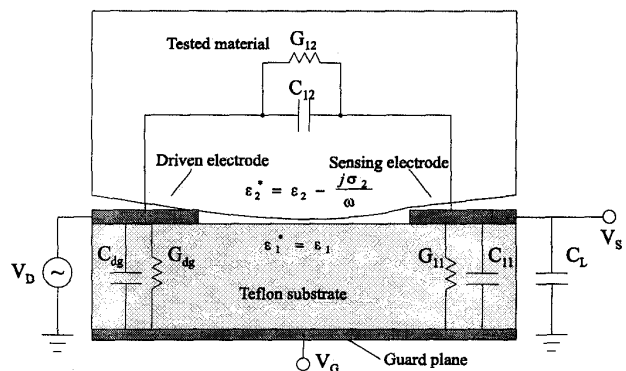


Figure 2. The cross-section of half-wavelength of an interdigital sensor.

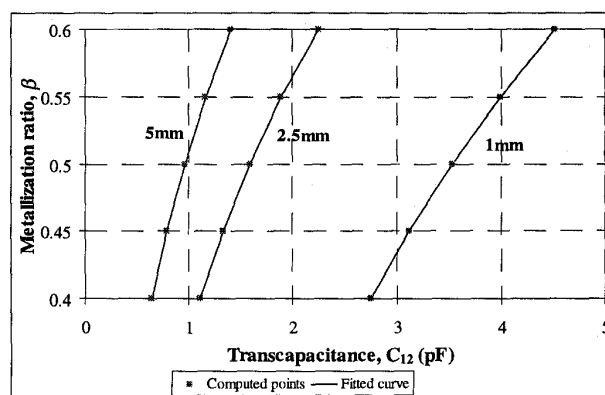


Figure 3. For all wavelengths, the interelectrode transcappacitance grows with the metallization ratio.

Table 1. Coefficients for the empirical relation (1).

Wavelength	$a_2$	$a_1$	$a_0$
$\lambda=1.0 \text{ mm}$	0.7934	-0.0966	-0.6502
$\lambda=2.5 \text{ mm}$	0.8419	-0.1545	-0.3157
$\lambda=5.0 \text{ mm}$	0.9099	-0.1954	-0.2040

### Interpolation Curves

After the metallization ratio,  $\beta$ , is determined, the sensor is ready for measurements. Let us first consider the simplest case: a non-conducting homogenous fluid above the sensor. For each wavelength, we calculated the dependence of the capacitance on the relative dielectric permittivity,  $\epsilon_r$ , of the tested material. Figure 4 shows the inverse dependence  $\epsilon_r(C_{12})$  plotted for several values of the metallization ratio  $\beta$  for the 1 mm wavelength. The curves for the other two wavelengths have similar shapes.

Thus, since the numerical value of  $\beta$  is known from the calibration in air, we can easily find the relative dielectric permittivity  $\epsilon_r$  from the measured value of  $C_{12}$  by interpolating the curves in Figure 4. The choice of the interpolation

technique is not crucial. We use functional approximation, although other methods, such as look-up tables, could have been used. For each wavelength, we approximate the family of curves such as shown in Figure 4 by the equation

$$\epsilon_r = b_2(\beta)\sqrt{C_{12}} + b_1(\beta)C_{12} + b_0(\beta), \quad (2)$$

where the variable coefficients  $b_2(\beta)$ ,  $b_1(\beta)$ , and  $b_0(\beta)$  are found from the finite-element simulation. These coefficients, in turn, are approximated with the second-degree polynomial:

$$b_i = c_{2,i}\beta^2 + c_{1,i}\beta + c_{0,i}. \quad (3)$$

Figure 5 shows the functional dependencies of these coefficients on the metallization ratio  $\beta$  for the 1 mm wavelength. The remaining functions have similar shapes and can be found using the coefficients listed in Table 2. The expressions (2) and (3) are only applicable for fluid dielectrics. The air gap, which forms between the sensor and the surface of the solid material, reduces the interelectrode capacitance. Figure 6 shows the effect of the air gap on the inverse functional dependence  $\epsilon_r(C_{12})$ . We account for this effect by using equations (2) and (3) for the fluids, and a linear fit of the  $\epsilon_r(C_{12})$  function for the solids. The intercept of the linear fit and the fluid curves at  $\epsilon_r=1$  are the same, and the slope is based on the derivative of the liquids curve at a point where  $\epsilon_r = 1$ . The angle  $\alpha$  between the tangent of the fluids curve and the solid materials curve is 0.096 rad, 0.041 rad and 0.0002 rad for 1 mm, 2.5 mm, and 5 mm wavelengths, respectively.

### Purely Capacitive Measurements

The measurement of the real part of the complex dielectric permittivity with the imaginary part being negligible is a conceptually simple task. However, previous measurements with interdigital sensors indicated significant differences between the predicted and the measured values. This section illustrates the performance of the sensor for low conductivity dielectrics. Table 3 lists the results of measurements made on a variety of fluid and solid homogeneous dielectrics. For a homogeneous material, all three wavelengths should indicate approximately equal values of  $\epsilon_r$ , and each of them should be close to the value found with the parallel plate capacitor measurements. For solid materials, these measurements were done with guard ring electrodes deposited on the surface of specimens in accordance with ASTM standard [4]; and for liquid materials, they were done by immersing the parallel plate capacitor into the liquid. The air measurement is guaranteed to be perfect by the nature of the calibration procedure.

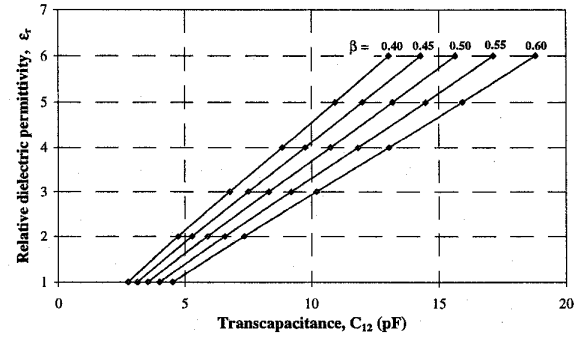


Figure 4. Effect of the electrode width is calculated for distinct values of the metallization ratio (from 0.4 to 0.6) and later interpolated for the 1 mm wavelength.

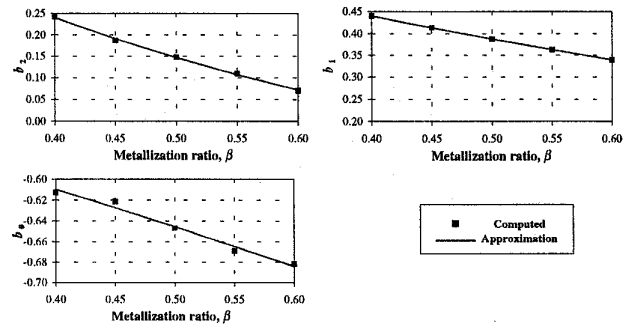


Figure 5. Coefficients for 1 mm wavelength describing the relation between  $\epsilon_r$  and  $C_{12}$  are dependent on  $\beta$ .

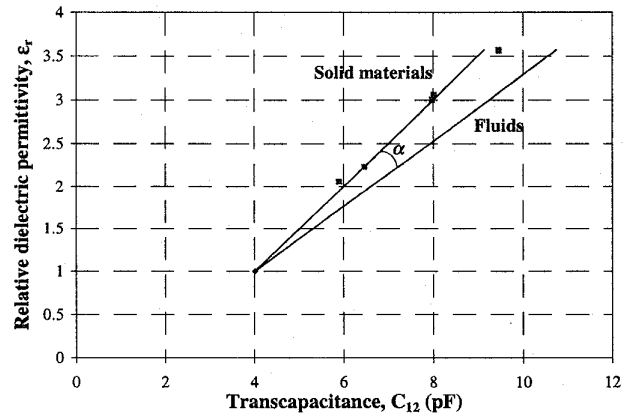


Figure 6. Influence of the air is accounted for by assuming a small angle  $\alpha$  between the two linear approximations of the sensor response. The “Fluids” line is found by finite-element simulations and the “Solid materials” is empirical.

Table 2. Coefficients for the relations (2) and (3).

	$\lambda=1\text{mm}$			$\lambda=2.5\text{mm}$			$\lambda=5\text{mm}$		
	$b_2$	$b_1$	$b_0$	$b_2$	$b_1$	$b_0$	$b_2$	$b_1$	$b_0$
$c_2$	0.929	0.209	-0.126	2.299	0.186	-0.268	3.511	0.187	0.931
$c_1$	-1.773	-0.715	-0.247	-4.594	-0.617	0.396	-7.109	-0.575	-0.428
$c_0$	0.801	0.693	-0.490	2.277	0.653	-0.451	3.718	0.610	-0.394

**Table 3. Measurement of relative dielectric permittivity of non-conductive materials in 100 Hz -10 kHz range .**

Material	1mm	2.5mm	5mm	Average	Parallel plate
Air	1.00	1.00	1.00	1.00	1.00
Teflon	1.92	2.03	2.02	1.99	2.06
Transformer oil	2.23	2.29	2.27	2.26	2.20
Polyethylene	2.24	2.26	2.29	2.26	2.23
Polypropylene	2.35	2.35	2.29	2.33	2.35
HD Polyethylene	2.38	2.44	2.38	2.40	2.36
Lexan	3.11	3.04	3.11	3.09	3.01
Corn Oil	3.09	3.19	3.10	3.13	3.10
PVC	3.30	3.23	3.45	3.32	3.35
Delrin (white)	3.36	3.49	3.77	3.54	3.63

### Simulation and Measurements for a Wide Frequency Range

Fast evaluation of the complex dielectric constant is possible by extending the described approach to a larger number of variables. Such an approach is currently being developed. Meanwhile, a slower algorithm, based on the iterative guess of the material properties can be used. In both cases, it is necessary to verify that the finite element simulation performs adequately for all studied cases.

Figure 7 shows the results of a frequency sweep simulation and measurements with the sensor immersed in corn oil. The values of the relative dielectric permittivity  $\epsilon_r=3.15$  and conductivity  $\sigma=60$  pS/m, 53 pS/m, and 14.2 pS/m for 1 mm, 2.5 mm, and 5 mm wavelengths, respectively, used in the simulation were measured separately with a parallel plate sensor. The values of the conductivity are different because the measurement with each wavelength were taken at different moments of time at different ambient temperatures which varied between 15°C and 25°C.

Corn oil is non-dispersive in this frequency range (0.005 Hz to 10 kHz). A good agreement between the experimental and the theoretical values is achieved. Low frequency data differ due to the capacitive double-layer effect, which is currently not included in the model. The negative value of the transcapacitance at low frequencies is due to the actively driven three-terminal arrangement, and does not contradict any circuit laws [3].

### Conclusions

Improvements of interdigital dielectrometry measurement techniques are discussed. The precision and speed of previously developed parameter estimation algorithms are increased by introducing a self-calibrating procedure into a model-based measurement of dielectric properties of insulating materials.

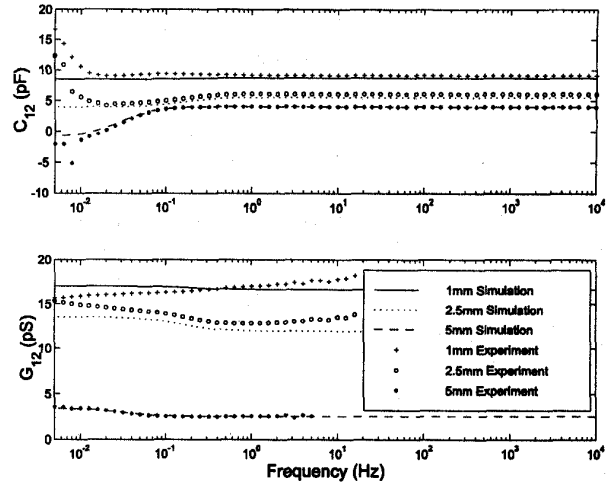


Figure 7. Comparison of measured and calculated interelectrode transcapacitance  $C_{12}$  and transadmittance  $G_{12}$  for the experiments with corn oil.

Comparison between the measurements and the finite-element simulation confirms adequacy of the selected model. Future work will extend the described approaches to more complicated cases, where properties of non-homogeneous materials of arbitrary configurations will be estimated with interdigital dielectrometry sensors.

### Acknowledgments

The authors would like to acknowledge the support of the Electric Power Research Institute, under grant WO 3334-1, managed by Mr. S. Lindgren, and the National Science Foundation under grant No. ECS-9523128. The donation of Maxwell software by Ansoft Corp. is gratefully appreciated. The authors would like to thank MIT graduate students Darrell Schlicker and Yanko Sheiretov for valuable discussions

### References

1. Zaretsky, M.C., Mouayad, L., and Melcher, J.R., "Continuum Properties from Interdigital Electrode Dielectrometry," *IEEE Transactions on Electrical Insulation*, Vol. 23, No.6, December 1988, pp. 897-917.
2. von Guggenberg, P.A., and Melcher, J.R., "A Three-Wavelength Flexible Sensor for Monitoring the Moisture Content of Transformer," *Proceedings of the 3rd International Conference on Properties and Applications of Dielectric Materials*, July 1991, pp. 1262-5.
3. A.V. Mamishev, B.C. Lesieutre, M. Zahn, "Optimization of Multi-Wavelength Interdigital Dielectrometry Instrumentation and Algorithms," submitted to *IEEE Transactions on Dielectrics and Electrical Insulation*.
4. AC Loss Characteristics and Permittivity (Dielectric Constant) of Solid Electrical Insulating Materials," *Annual Book of ASTM Standards*, D150-81.